D.C. Vadillo, S.D. Hoath, W-K. Hsiao, M.R. Mackley, in Proc 27th Int. Conf. on Digital Printing Technologies, NIP27, Minneapolis, MN, USA, 2011, 568-572, 'The effect of inkjet ink composition on rheology and jetting behaviour'

The effect of inkjet ink composition on rheology and jetting behavior

Journal:	*NIP and Digital Fabrication 2011*
Manuscript ID:	124
Presentation Type:	Oral
Date Submitted by the Author:	04-Jul-2011
Complete List of Authors:	Vadillo, Damien; University of Cambridge, Chemical Engineering Hoath, Stephen; University of Cambridge, Engineering Hsiao, Wen-Kai; University of Cambridge, Engineering Mackley, Malcolm; University of Cambridge, Chemical Engineering

The effect of inkjet ink composition on rheology and jetting behaviour

Damien C Vadillo[1], Stephen D Hoath[2], Wen-Kai Hsiao[2] and Malcolm R. Mackley[1]*

[1]*Department of Chemical Engineering and Biotechnology, University of Cambridge, Cambridge, United Kingdom*

[2]*Institute for Manufacturing, Department of Engineering, University of Cambridge, Cambridge, United Kingdom*

Abstract

This work presents recent results on the way linear and non linear viscoelastic properties of the fluids affect the jetting mechanism. Recent progress on quantitative characterising both high frequency linear (LVE) and non-linear (NLVE) viscoelasticity of fluids allows fluids to be assessed for their jettability before using such materials in a DoD print head. In term of linear viscoelastic measurements, the Piezo Axial Vibrator (PAV) was used to probe the rheology of the fluids on a frequency range between 10Hz and 10000Hz. A filament stretching apparatus, called the "Cambridge Trimaster", was used in combination with high speed cinematography, to characterize the fluids high speed stretching and break-up behaviour. The series of fluids investigated here consist in dilutions of mono disperse polystyrene with different molecular weight (110, 210, 306 and 488 kg/mol respectively) diluted in diethyl phthalate. The choice of polymer weights and concentrations were chosen to match both the complex viscosity and the LVE. However, non linear rheological data experiments exhibit differences in the fluid relaxation time and filament break-up mechanism. Ultra-high speed cinematography of DoD jetting events were correlated with filament break-up experiments and demonstrated that fluid rheology provides valuable information on the jetting quality of the fluids.

Introduction

Liquid droplet formation is relevant to several applications where the deposition of a controlled volume of fluid on a specific location is required. Inkjet printing [1], Organic Light Emitting Diode (OLED) [2] fabrication or Deoxyribonucleic Acid (DNA) [3] in situ synthesis are examples. Different techniques can be employed to form a droplet and piezo-type Drop-on-Demand is one of the most recent. This method consists in creating a pressure wave within a micro-capillary channel full of liquid with an orifice at one end with a typical diameter D_0 of 20 to 50 μm. Piezo-electric wall actuators generate a pressure wave which acts against the fluid viscosity and surface tension. A ligament of liquid is ejected from the orifice and subsequently breaks into droplets [4].

Droplet formation is influenced by both the physical properties of the ejected fluid and the process itself. The fluid density ρ, viscosity η and surface tension σ are relevant and typically the viscosity is between 1 to 20 mPa.s at temperature between 25°C and 50°C and surface tension 20 to 40 mN/m for ink-jet applications. The amplitude of the pulse applied on the fluid also influences the jetting by modifying the fluid velocity U outside the printhead. From dimensional analysis, the Reynolds number, which represent the ratio of the inertia to viscous force, and the Weber number, which represent the ratio of the inertia to surface tension force, have been found to control the jetting process [5]. They are defined as following:

$$\mathrm{Re} = \frac{\rho D_0 U}{\eta} \quad (1)$$

$$\mathrm{We} = \frac{\rho D_0 U^2}{\sigma} \quad (2)$$

The Ohnesorge number, which represents the ratio of viscous to surface tension forces and which is independent of the droplet velocity, also plays an important role. It is defined as following

$$\mathrm{Oh} = \frac{\eta}{\sqrt{\rho D_0 \sigma}} \quad (3)$$

Fromm [5] predicted that stable droplet formation can occur for $Z > 2$ where Z is the inverse of the Ohnesorge number. Later, a computational and experimental study about the DOD drop formation by Reis and Derby [6] showed that a printable fluid should obey $1< Z <10$. The lowest value of Z is governed by the dissipation of the pressure wave by the viscosity of the fluid whereas the higher limit is determined by the fact that the fluid forms satellites droplet instead of a unique droplet. These past studies of DOD jetting have only considered Newtonian fluids, however, it has been established that viscoelasticity can strongly influence ink-jet performance [8]. Ink-jet fluid linear viscosity can be represented in term of a Complex viscosity $\eta^* = (G' + iG'')/\omega$ where G' is the elastic modulus and G'' is the loss modulus. Previous work has shown that inkjet fluids can be characterised using G' and G'' data, however, the short relaxation times involved with ink jet fluids require special experimental techniques to be adopted [8, 9].

In the present work, LVE and NLVE of matched viscosity polymer solution were investigated using Piezo Axial Vibrator (PAV) [10] and the "Cambridge Trimaster" filament stretching apparatus [11] respectively. The rheological data measured on these fluids have been correlated with high speed picture of the jetting mechanism.

Experiment; fluids and apparatus

Four solutions of polystyrene (PS) with different molecular weight (110 kg/mol (PS110), 210 kg/mol (PS210), 306 kg/mol (PS306) and 488 kg/mol (PS488)) dissolved in diethyl phthalate (DEP) were prepared. The polymer concentration was adjusted in order to obtain a series of fluids with a matched complex viscosity of

about 16mPa.s at 20°C as well as high frequency linear viscoelastic modulus (see section results). To ensure the dilute character of these fluids, entanglement concentration c* at which the coils at equilibrium begin to physically overlap has been determined from measure of the intrinsic viscosity [η] (for a full details on the method please see [12]). The fluid physical properties are summarized in Table 1. The fluids of the constituted series had a density of 1120kg/m^3 and a surface tension of 37mN/m.

Fluid	M_w (kg/kmol)	c (w/w)	c* (g/ml)	η_0 (mPa.s)
I	110000	0.5	2.56	16.3
II	210000	0.4	2.24	16.5
III	306000	0.2	1.9	15.5
IV	488000	0.1	1.15	14.8

Table 1: Fluids physical parameters

The high frequency linear viscoelasticity (LVE) of the fluids were investigated using a Piezo Axial Vibrator (PAV) [10].

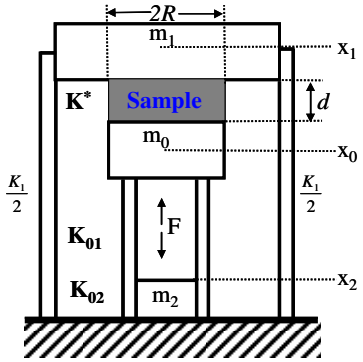

Figure 1: Mechanical Model of the PAV

The apparatus, schematically presented in figure 1, consists of a thin cavity of liquid (d < 200μm) surrounded by solid surfaces. An oscillatory piezo-element activated squeeze flow is generated by the motion of a bottom plate with a small amplitude of approximately 5nm over a range of frequency from 0.1Hz to 10000Hz. The complex spring constant K^* of the apparatus is first determined without the fluid being presented and then with the fluid present, the difference giving the response of the fluid on its own. The PAV gives the shear modulus, $G^* = G' + iG''$, and the complex viscosity $\eta^* = G^*/i\omega$ (where ω is in rad/s). The temperature is regulated in the PAV and a range between 5°C and 50°C can be investigated.

The second experimental set up is a filament stretching, extensional rheometer, the "Cambridge Trimaster" [11]. This apparatus performs filament stretching at a constant velocity for a fluid initially placed between two pistons of initial diameter 1.2mm. Both pistons, are attached on the opposite side of a belt, and move symmetrically apart for a given distance allowing the mid-filament to remain in a central position during the experiment. The pistons can moved from a distance of 10μm to 10cm at a maximum relative velocity of 1m/s. When the pistons stop, the filament self-thins under the action of the capillary and viscous forces. The Bond number was calculated to be small (Bo = $\rho g D_0^2/4\sigma$ = 0.1), confirming that gravitation effects were negligible in comparison to capillary forces.

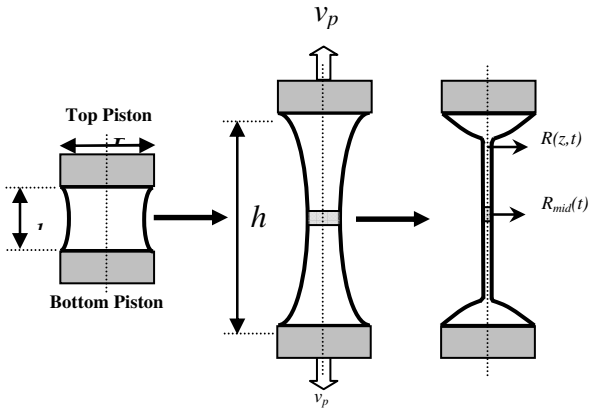

Figure 2: Schematic of the "Trimaster" filament stetching and breakup apparatus

A high speed camera (Photron Fastcam 1024 PCI) was coupled with the "Cambridge Trimaster", allowing the transient profiles to be recorded at a frame rate of 45000 frames per second but at the reduced resolution of 64x128 pixels, and with a shutter time as low as 3μs. The magnification was 5.5μm per pixel and the continuous light is guided by fibre optics. The filament thinning measurement, as well as the filament break-up behaviour, was obtained using automatic image treatment specifically developed for, and included within, the "Cambridge Trimaster" software suite. This apparatus enables the measurement of the transient elongational viscosity and the observation of filament profiles. Both elements are relevant to inkjet droplet and satellite formation.

The jet imaging rig, as shown in Fig. 3, consists of a Shimadzu HPV-1 ultra high-speed camera which is capable of capturing 102 full resolution (310 X 260 pixels) gray scale images at 1,000,000 fps with exposure time down to 0.25 μs. The illumination was provided by an Adapt Electronics Photoflash system which produces 2 ms duration, 500 Joules flashes. Due to the finite warm up time of the light source and consequent strong variation in the illumination, the triggers for the print head firing and camera were delayed (~ 100μs) relative to the trigger to the light source controller (CU-500), using a delay generator (TTi TGP-110). A see-through glass nozzle (MicroFab MJ-ABP-01-30-6MX) was mounted vertically on a motorized multi-axis positioning stage with its (guarded) nozzle directed downwards between the camera and the flash. The camera, fitted with a microscope lens (Navitar 12X ultra zoom with Mitutoyo objectives with long working distance), records shadowgraph images of the fluid lying either within the 30 μm diameter nozzle exit or outside in the jet. The images captured by the Shimadzu camera are in a proprietary format, which was subsequently converted to either AVI format movies or individual TIFF files for our further off-line analyses. In order to show the influence of the elasticity and finite length of the polymer molecules involved on the evolution of the jet velocity and break up, the print head drive setting used was identical for each fluid.

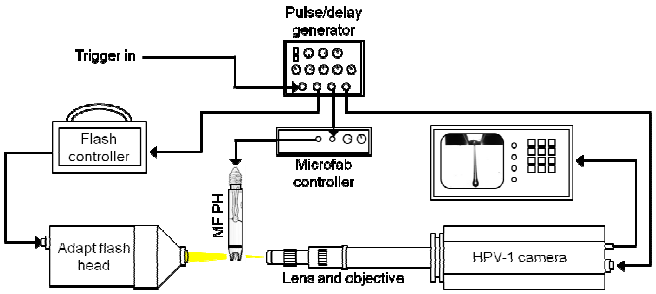

Figure 3: Schematic of the nozzle imaging system used in the present work.

Results and discussion

PAV: Linear viscoelasticity.

Fig. 4 presents linear viscoelastic PAV data of viscous and elastic modulus response as a function of frequency for the fluids investigated here. G'' data exhibit a perfect superposition for the four samples tested as well as a linear increase with frequency. In terms of elastic components, G' data also show relatively good match, despite a magnitude at least one order of magnitude lower than G'' data, and a development with frequency following a gradient close to two. These results indicate both that match complex viscosity fluids have been formulated and that the complex viscosity is independent of the frequency. The PAV data also demonstrate that the formulated fluids are viscoelastic at high frequency (relevant to ink jet printing process) and that they are perfectly identical in terms of LVE behaviour. As a consequence, no distinction between them can be made from only LVE measurements although relaxation spectrum can be extracted.

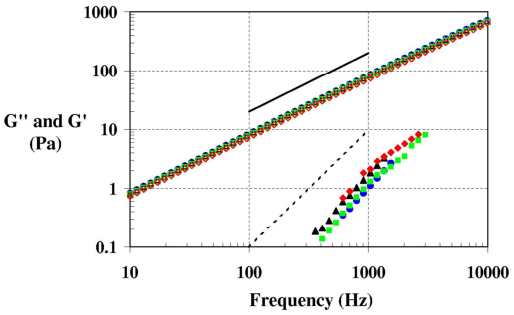

Figure 4: Loss modulus G'' and elastic modulus G' of the solution of DEP-PS at different weight concentration and polymer molecular weight, η* ~ 16mPa.s at 20°C. The full and dash lines are guides and represents an evolution with slope of 1 and 2 with the frequency respectively. Fluids (●) I, (▲) II, (■) III and (♦) IV

The behaviour of G' and G'' captured here is consistent with low frequency limit of Maxwell or Zimm model. Zimm model, as described by equation 4 and 5 is usually preferential to a Maxwell model in the literature for the case of dilute polymer samples. It is, therefore, the one selected here.

In this model, the polymer contribution to both the elasticity and viscosity of the sample is added to the solvent contribution. In the case of Newtonian solvent, such as DEP, the solvent only contributes to the loss modulus G'' and is represented here by the term $\eta_s\omega$ in eq. 5.

In these equations, c is the concentration of polymer, where R = 8.314 J/mol.K is the universal gas constant, ω is the angular frequency, T is the absolute temperature, $\tilde{\sigma}$ is the measure of the hydrodynamic interaction between the segments of the polymer chain and the surrounding solvent [12] and *i* represents the mode number. Fitting this model, in the limit of mono mode description (G' ~ f^2 and G'' ~ f), to the experimental data presented in Fig. 4 enables the extraction of the Zimm longest relaxation time λ.

$$G'(\omega)=\frac{cRT}{M_w}\sum_{i=1}^{N_{modes}}\left(\frac{(\lambda\omega)^2}{i^{4+2\tilde{\sigma}}+(\lambda\omega)^2}\right) \quad (4)$$

$$G''(\omega)=\eta_s\omega+\frac{cRT}{M_w}\sum_{i=1}^{N_{modes}}\left(\frac{(\lambda\omega)i^{2+\tilde{\sigma}}}{i^{4+2\tilde{\sigma}}+(\lambda\omega)^2}\right) \quad (5)$$

Longest Zimm relaxation time of 8.7μs, 29μs, 41μs and 88μs have been measured for fluids I to IV respectively. These results are in agreement with reported results where polymer Zimm relaxation time scale with $M_w^{3\upsilon}$, with υ ~ 0.55 for polystyrene in DEP [13]. It should also be mentioned that, using a mono mode Maxwell model leads to similar relaxation time than the one obtained using the Zimm model. Both approaches are equivalent here.

Cambridge Trimaster: Non linear viscoelasticity

The fluid rheological response to a large deformation (non linear regime) can be probed by filament stretching and thinning experiments where the evolution of the mid filament is related to the transient extensional viscosity η_{ext} by [14]:

$$\eta_{ext}=-\frac{(2X-1)\sigma}{dD_{mid}(t)/dt} \quad (6)$$

where X is an adjustable parameter that includes the deviation of the filament from the slender hypothesis and σ is the fluid surface tension. The competition between the fluid surface tension, which is the driving thinning force, and its viscosity and the elasticity (which stabilise the filament) results in different thinning behaviour. In the case of a Newtonian fluid, D_{mid} evolves proportionally to α.t (with α < 0) whereas an exponential decay is observed for viscoelastic fluids (D_{mid} ~ β.exp(-t/3λ_{ext} and where λ_{ext} is the longest extensional relaxation time).

Filament thinning experiments can be used to extract the fluid extensional behaviour as well as investigate the drop break up [12,13,14]. High speed photograph of the filament thinning are presented in Fig. 5 where the effect of polymer molecular weight is visible. The formation of a long lasting thin thread, located on the top and the bottom of the filament, are visible and their size increase with polymer molecular weight. The formation of bead on string is also visible for the fluid IV. This capability of the fluid to extend is expected to have a strong influence on the jetting behaviour (see section below). In this figure, the break up time has been chosen as the time reference due to the incapacity of recording the full piston (picture size 64x128 at 45000fps).

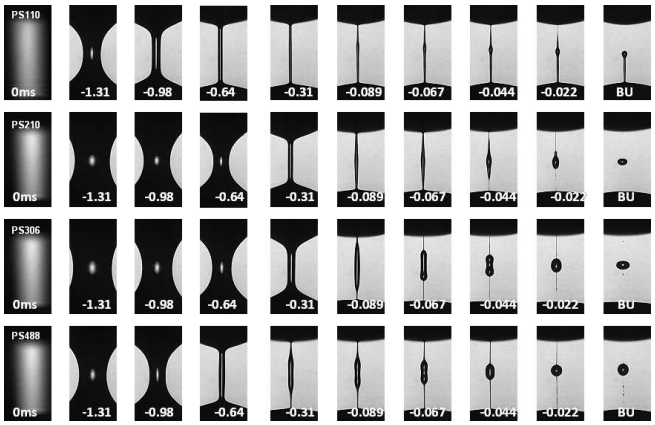

Figure 5: Photograph of the filament break up with the Trimaster of mixture of fluid I to IV from top to bottom respectively. Initial gap size: 600µm, stretching distance: 800 µm (final gap size: 1400µm), piston speed: 150mm/s, capture frame rate: 45000 fps, exposure time: 3µs.

It should be noticed here that all break up dynamics occurred in less than 600µs making again difficult to differentiate the fluids. Photographs presented in Fig. 5 can only be obtained under very specific experimental conditions due to the fluids used and the subtlety of the mechanism investigated. These conditions are specified in the figure caption but the definition of these conditions is not discussed here. The stress that growth in the filament was sufficient to stretch the polymer molecules and hold an elasto-capillary regime although this latest was located on the top and bottom of the filament. The evolution of the smallest filament width has then been used in eq. 6 to extract a filament thinning relaxation time. The evolution of D_{min} are presented in Fig. 6 where the transition between inertio-capillary regime ($D \sim \alpha.t$) and elasto-capillary regime ($D_{mid} \sim \beta.\exp(-t/3\lambda_{ext})$) is visible for all the fluids.

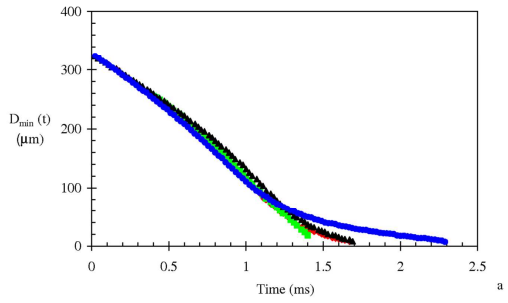

Figure 6: Evolution of the minimum diameter as a function of time for fluids (●) I, (▲) II, (■) III and (♦) IV

Fitting an exponential evolution for D_{min} on data presented in Fig. 6 enabled filament extensional relaxation time of 197µs, 92µs, 29.5µs and 83µs to be extracted for fluids I to IV respectively. These results demonstrated that filament stretching experiments, when performed under relevant experimental conditions can access fluid extensional relaxation on the time scale commensurable with Drop on Demand jetting mechanism. It is also important to notice the fluid extensional relaxation time can be significantly larger than the longest Zimm relaxation time. As an example, the ratio of relaxation time λ_{ext} / λ_z has been found to be larger than 20 for fluid I. This demonstrates that the level of diluteness of a fluid can be different in shear and in uni-axial extensional flow which has subsequent important implication for micro droplet formation mechanism.

Jetting: high speed imaging of droplet formation

Figures 7 and 8 show narrow strips taken from high speed images of the fluid jetting from the 80µm diameter MicroFab nozzle; the nozzle exit is at the top of each strip and they are to the same scale.

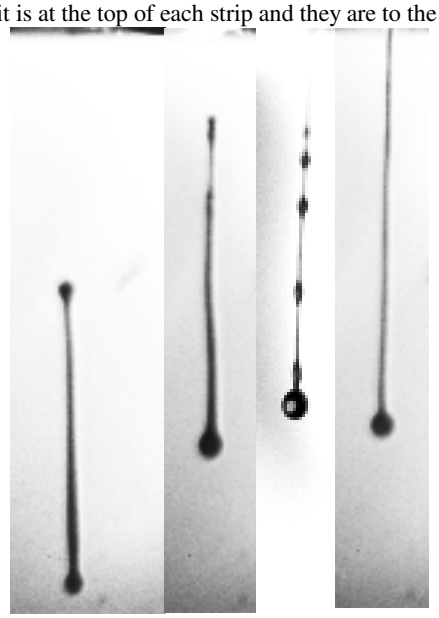

Figure 7: Ultra high speed images (500,000 fps) obtained with a MicroFab nozzle drive amplitude of ±35V and jetted solutions (a) DOP (10%)/DEP (90%) after 145µs, (b) PS110 (0.5%) after 145µs, (c) PS306 (0.2%) after 200µs and (d) PS488 (0.1%) after 200µs

Figure 7 presents the droplet profile for 4 different fluids; (a) DOP (10%) / DEP (90%) after 145µs, (b) PS110 (0.5%) after 145µs, (c) PS306 (0.2%) after 200µs and (d) PS488 (0.1%) after 200µs. The solvent mixture (7(a)) and the PS110 (0.5%) fluid (7(b)) have broken off from the meniscus on the timescale of the images whereas the PS306 (0.2%) and the PS488 (0.1%) fluids are still attached to the nozzle even later. Nonetheless, differences are also visible with formation of beads on string for PS306 (0.2%) whereas PS488 (0.1%) exhibits a cylindrical ligament (Fig. 7(c) and 7(d)). The different jetting behaviour of these polymer fluids is therefore determined partially but significantly by their non-linear viscoelasticity because they have very similar linear viscoelasticity. A clear requirement to more fully characterise inkjet fluids is seen. Figure 8 shows part of the timed high speed image sequence for a single jetting event for PS488 (0.1%) fluid, with the cylindrical ligament at (a) shown as a visual reference after 200µs, being a repeat of that shown in Fig. 7(d). The ligament is still attached after 320µs as shown by 8(b), but has beads on the string forming. The ligament ruptures at the midpoint in 8(c) and has completely retracted between beads and the nozzle in 8(d) only 20 µs later, and has caused elastic recoil motion of the leading satellite in 8(e).

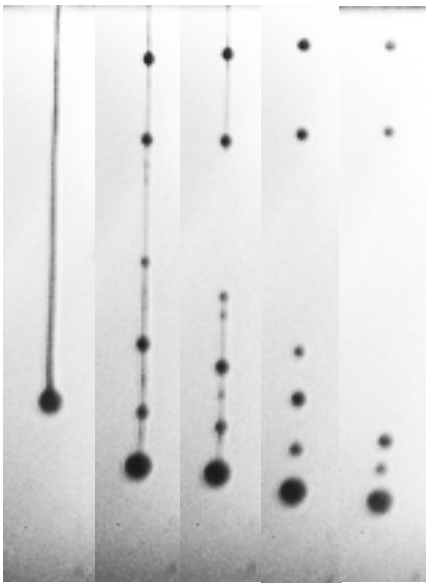

Figure 8: Timed image sequence for PS488 (0.1%) jetted with ±35V drive; (a) after 200µs, (b) after 320µs, (c) after 340µs, (d) after 360µs, (e) after 400µs.

Again, the correspondence between the jetting behaviour in Fig. 7 and 8 and the rheological testing results in Fig. 5 and the corresponding analyses in Fig. 6 is very clear and striking and show the relevance of filament thinning experiments in the characterisation of inkjet ink jetting quality.

Conclusions

In this work, model inkjet polymer fluids with different polymer concentration and molecular weight have been formulated. Fluids rheology have been characterised under Drop on Demand flow conditions, namely in high frequency linear regime using the Piezo Axial Vibrator and non linear deformation regime using the Cambridge Trimaster. Results demonstrated that fluids complex viscosity and linear viscoelasticity have been matched. Extensional rheology tests had shown significant differences in the filament break up process with the apparition of longer lasting filament on which beads can develop as the polymer molecular weight increased. In addition, the shear rheology relaxation time has been found to be significantly shorter than the extensional relaxation time. These data have been correlated with the jetting with fixed jetting conditions. The pattern observed on filament stretching photographs has also been observed in jetting with filament that elongates as the polymer molecular weight increased, forms more satellites as well as droplet slow down. This study demonstrates that fluids level of diluteness, and subsequently behaviour, varies with the type of flow. As a consequence, investigating both high frequency linear viscosity and non linear viscosity (under carefully selected conditions) prior to the ejection can be used to accurately predict fluids behaviour during ejection.

References

[1] Stanton D. W. and Rutland C. J., "Multi-dimensional modeling of thin liquid films and spray-wall interactions resulting from impinging sprays", Int. J. of Heat and Mass Transfer, 41, 3037-3054 (1998).

[2] C-T Chen, Tseng FG and Chieng CC, "Evaporation evolution of volatile liquid droplets in nanoliter wells", Sensors and Actuators, **130–131**, 12–19 (2006)

[3] Beier M. and Hoheisel J. D., "Analysis of DNA-microarrays produced by inverse in situ oligonucleotide synthesis", J. of Biotech., **94**, 15–22 (2002)

[4] L. Rayleigh, "On the instability of jets", Proc. London Math. Doc., 10, 4 (1879).

[5] J.E. Fromm, IBM J. Res. Dev., **28**, 322-333 (1984.

[6] Reis and Derby, B. Mater. Res. Soc. Symp. Proc., **625**, 117-122 (2000).

[7] D. Jang *et al.*., "Influence of fluid properties on Ink-jet printability", Langmuir, **25**, 2629-2635 (2009).

[8] TR Tuladhar, MR Mackley, J. Non-Newtonian Fluid Mech., 148, 97-108 (2008).

[9] S.D. Hoath *et al.*, "Link between ink rheology, drop-on-demand jet formation and printability", J. Imaging Sci. Tech., **53**, (2009).

[10] J. Crassous *et al.*, "Characterisation of the viscoelastic behaviour of complex fluids using the piezoelastic axial vibraor", J. Rheol., **49**, 851-863 (2005).

[11] DC Vadillo *et al.* , "The development of the "Cambridge Trimaster" filament stretch and break-up device for the evaluation of ink jet fluids", J. Rheol, submitted (2009).

[12] Clasen *et al.*, "How dilute are dilute solutions in extensional flows?", J. Rheol., **50(6)**, 849-881 (2006).

[13] Anna S.L. *et al.*, "An interlaboratory comparison of measurements from filament-stretching rheometers using common test fluids", J. Rheol., **45**, 83–114 (2001).

[14] McKinley G.H. and A. Tripathi, "How to extract the Newtonian viscosity from a capillary break up measurement in a filament rheometer", J. Rheol, **44**, 653-670 (2000).

Acknowledgements

The authors would like to thank the Engineering and Physical Sciences Research Council (UK) and industrial partners in the Innovation in Industrial Inkjet Technology project, EP/H018913/1 for financial support.

Author Biography

Damien Vadillo is currently an associate researcher in the Department of Chemical Engineering and Biotechnology in the University of Cambridge (UK). He works on the effect of high frequency viscoelasticity of inkjet fluids on their jet-ability, and filament break-up behaviour. He has a PhD degree from the University Joseph Fourier of Grenoble (France) that he completed in 2007 on the characterisation of the hydrodynamic phenomena during drop impact onto different types of substrates.

** The paper will be presented by Stephen Hoath.*